The Advances in Conversion Techniques in Triboelectric Energy Harvesting A Review

Peng, Wenyu; Du, Sijun

DOI
10.1109/TCSI.2023.3261780

Publication date
2023

Document Version
Final published version

Published in
IEEE Transactions on Circuits and Systems I: Regular Papers

The Advances in Conversion Techniques in Triboelectric Energy Harvesting: A Review

Wenyu Peng, *Student Member, IEEE*, and Sijun Du, *Senior Member, IEEE*

***Abstract*— A triboelectric nanogenerator (TENG) is a new transducer utilizing contact electrification and electrostatic induction to transform mechanical energy into electric energy. Due to its high energy density and flexibility, it can be employed to make electronic devices self-powered by harvesting ambient mechanical energy in many application scenarios, such as biomedical devices, wearable electronics, and Internet-of-Things (IoT) sensors. However, due to the time-varying and low internal capacitance of a TENG, it is challenging to extract electrical energy from it. Hence, good power conversion techniques are crucial in TENG energy harvesting systems. Currently, studies on dedicated integrated power conversion techniques are very limited. Due to the exponentially increasing research interests in TENG, a comprehensive study on the TENG energy harvesting system, emphasizing integrated-circuit (IC) power conversion techniques, is urgently needed. This paper summarizes and compares the state-of-the-art triboelectric energy harvesting systems, focusing on different power conversion techniques for output power enhancement. Some techniques, which have been widely used in other relevant energy harvesting systems, are also mentioned to inspire innovative design strategies for TENG systems.**

***Index Terms*— Power management, triboelectric, transducer, rectifier, switched-capacitor converter, synchronous switching, MPPT.**

I. Introduction

CURRENTLY, electronic devices, e.g., Internet-of-Things (IoT) and biomedical devices, are widely used to make people's life smarter and easier. Most of them are powered by batteries, which will run out of energy eventually. Thus, battery-free systems have drawn much research interest in the past decade with energy harvesting technology, which harvests ambient sustainable energy and converts it into usable electrical form. Due to the ubiquity of kinetic energy, interest in kinetic energy harvesting dramatically increased in past decades. Piezoelectric energy harvesting is one of the most popular techniques for harvesting kinetic energy. It transduces mechanical movement/vibration into electricity, relying on the vibration of internal cantilevers or plates. Consequently, it can only provide high output power with periodic and stable mechanical vibration. However, many mechanical movements, such as human motions and tides, are irregular and unpredictable, leading to extremely low efficiency using piezoelectric energy harvesters. To harvest mechanical energy in much broader application scenarios, a new mechanoelectrical transducer was proposed recently: the triboelectric nanogenerator (TENG).

A TENG works based on triboelectrification (contact electrification phenomenon) and electrostatic induction. Triboelectrification refers to the redistribution of electric charges between two different substances when squeezed or rubbed against each other. When the distance or contact area between them changes, an electric potential will be induced due to the displacement current generated by the displacement of the static charge [1]. This indicates the potential of triboelectrification in sensing displacement and transducing mechanical energy to electric energy.

The first TENG was proposed in 2012 [2]. In recent years, the research interest in triboelectric energy harvesting has been exponentially increasing [3]. TENG is advantageous in high flexibility and energy density, making it more suitable for miniaturization and planarization than piezoelectric and electrostatic energy harvesters [4], [5], [6]. Different from piezoelectric and electromagnetic kinetic energy harvesting, triboelectric energy harvesting is not limited by the resonant frequency and thus can transduce more power at low and non-periodic vibration frequency [7], [8]. As a consequence, it has been experimentally validated to harvest mechanical energy from the human body when embedded in textile [9], or bracelet [10], [11], or even from the motion of organs [12] to provide a stable power supply to low-power wearable or implantable devices, such as IoT environment monitors [13], health monitors [14], [15], [16], [17], [18], [19], and human-machine interfaces [20], [21], [22]. Furthermore, the feasibility of TENG in harvesting tide energy, wave energy [23], [24] and wind energy [25], [26] has been exploited.

However, energy extraction from TENG with conventional circuits is difficult due to its time-varying high internal impedance. The integrated circuit (IC) technology provides the possibility and potential in enhancing energy extraction and harvesting from TENG, thanks to small leakage current and fully custom control designs. It has been widely implemented in power management and energy harvesting, with many efficient conversion techniques developed. However, despite many studies on TENG structures and applications, few studies have been devoted to providing a comprehensive overview of the IC power conditioning circuit for triboelectric energy harvesting. Due to the increasing research interest in designing

Manuscript received 21 December 2022; revised 11 February 2023 and 6 March 2023; accepted 22 March 2023. Date of publication 29 March 2023; date of current version 28 June 2023. This article was recommended by Associate Editor Y. Tang. *(Corresponding author: Sijun Du.)*

The authors are with the Department of Microelectronics, Delft University of Technology, 2628CD Delft, The Netherlands (e-mail: sijun.du@tudelft.nl).

Color versions of one or more figures in this article are available at https://doi.org/10.1109/TCSI.2023.3261780.

Digital Object Identifier 10.1109/TCSI.2023.3261780

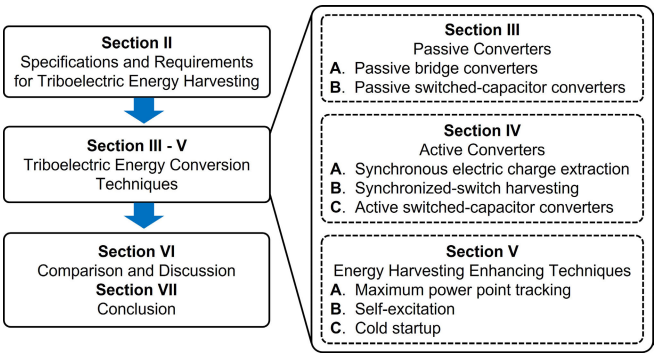

Fig. 1. The main contents organization of this review.

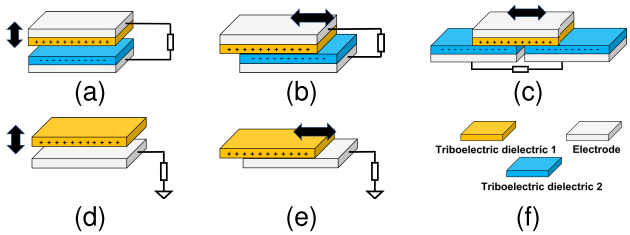

Fig. 2. Two electrode configurations for TENGs in different working modes: double-electrode configuration in (a) vertical contact-separation mode, (b) lateral-sliding mode, and (c) freestanding mode; Single-electrode configuration in (d) vertical contact-separation mode, and (e) lateral-sliding mode [28]. (f) Figure legends.

TENG-based systems, a review of the state-of-the-art IC conversion techniques and associated circuits is needed to inspire new harvesters for TENG. Thus, this review will start with a summary of the TENG features and energy harvesting specifications in Section II. Then the IC conversion techniques are categorized and introduced, in turn, from the simple passive configuration (Section III) to the complicated active configuration (Section IV). Apart from the converters, advanced integrated techniques to further enhance triboelectric energy harvesting performance are necessary and will be presented in Section V. After the introduction to conversion techniques, a comparison table is expected in Section VI to compare their practical performance of them with the state-of-the-art. At last, a conclusion will be given. A diagram of the main content's structure is presented in Fig. 1

II. Requirements for Triboelectric Energy Harvesting

A. Fundamental Theories of TENG

1) Structures: The triboelectrification phenomenon generates static electricity on dielectric, whose polarity and quantity are determined by electron affinities of materials [27], [28]. The displacement of charges generates electrical potential, which contains energy to be harvested and utilized. Typically, a TENG has three working modes: vertical contact-separation mode, lateral-sliding mode, and freestanding mode. Besides, there are two electrode configurations: single-electrode and double-electrode [28]. The combinations of different working modes and electrode configurations are illustrated in Fig. 2.

The vertical contact-separation mode has two dielectrics, or one dielectric and one electrode plate, moving face to face as presented in Fig. 2a and Fig. 2b. Triboelectrification occurs when they are in contact and squeezed. When two plates move away from each other, a voltage potential difference is induced between them by the displacement current. In lateral-sliding and freestanding mode, the plates can have rotational or translational movement with the triboelectricity generated by rubbing [29]. For the double-electrode configurations presented in Fig. 2b and Fig. 2c, when the effective contact area between dielectrics changes, the charge on the non-overlapping region induces different potentials on the anode and cathode electrode plates. While for the single-electrode lateral-sliding TENG illustrated in Fig. 2e, the potential is induced by the charge on the dielectric at the overlapping area between the dielectric and the electrode. With the lateral-sliding and freestanding TENG, the kinetic energy in the parallel relative motion can be harvested. For single electrode configurations, the current flows between electrode and ground, so the ground can be set as either anode or cathode in this case [28].

In the rest of this section, the double-electrode configuration will be taken as an example for theoretical analysis, but both single- and double-electrode configurations have similar properties.

2) Feature Analysis and Modeling: To design energy harvesting circuits for a TENG, the characteristics of current and voltage generated from it must be taken into consideration. The real-time output of a TENG can be comprehensively described by the V-Q-x relationship with three variables: the voltage between electrodes V, the generated charge Q, and the relative displacement between the plates x [30]. Since the TENG in contact-separation mode and sliding mode have different characteristics, they should be analyzed separately. First, the V-Q-x relationship of the vertical contact-separation TENG is elucidated. Based on its working mechanism, it can be approximately considered as a variable capacitor with a uniform electric field between plate electrodes [31], [32]. Thus, the induced V is derived by the product of x and the electric field intensity mathematically. The internal electric field of TENG is the superposition of two electric fields, induced by the triboelectric charge and the Q on the electrode plates respectively. Therefore, the V-Q-x relationship of the vertical contact-separation TENG can be derived by the following equation:

$$V = -\frac{Q}{S\epsilon_0}\left(\frac{d_1}{\epsilon_{r1}} + \frac{d_2}{\epsilon_{r2}} + x\right) + \frac{\sigma x}{\epsilon_0} \tag{1}$$

where:

S is the plate size;

ϵ_0 is the vacuum permittivity.

d_1 and d_2 are the thicknesses of dielectric layers;

ϵ_{r1} and ϵ_{r2} are the relative dielectric permittivity of each dielectric layer;

σ is the surface charge density of the dielectric generated by the triboelectrification;

These variables and parameters are labeled in Fig. 3a. Regarding single-electrode contact-separation TENGs, Eq. 1 also works except that only one dielectric layer exists; hence, one of the d_1 and d_2 should be set to 0. Eq. 1 can also be expressed in another form:

$$V = -\frac{Q}{C_{TENG}} + V_{OC} \tag{2}$$

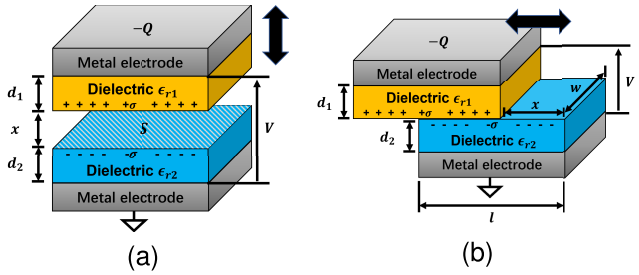

Fig. 3. The theoretical model of (a) the double-electrode vertical contact-separation TENG and (b) the double-electrode lateral-sliding TENG with significant parameters labeled [30], [33].

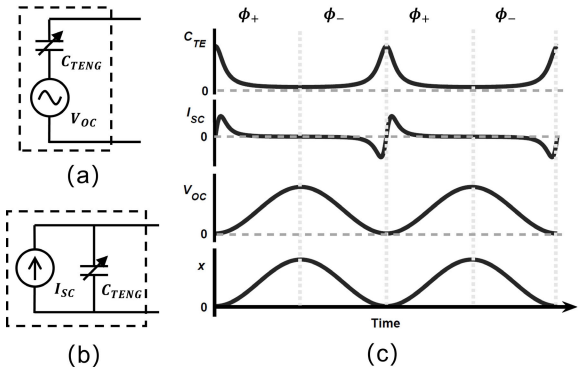

Fig. 4. (a) The theoretical equivalent voltage source model and (b) the theoretical equivalent current source model of TENG [34]. (c) The waveform of the real-time internal capacitance (C_{TE}), a current source (I_{SC}), and a voltage source (V_{OC}) are illustrated when TENG operates in sinusoidal vibration (x).

where,

$$C_{TENG} = \frac{S\epsilon_0}{d_0 + x} \qquad (d_0 = \frac{d_1}{\epsilon_{r1}} + \frac{d_2}{\epsilon_{r2}}) \tag{3}$$

$$V_{OC} = \frac{\sigma x}{\epsilon_0} \tag{4}$$

Another important parameter of TENG in analyzing the energy extraction efficiency is the maximal charge output, i.e., the total output charge under short-circuit conditions in each semi-cycle, denoted as Q_{SC}. Its relationship with x is derived from Eq. 1 with $V = 0$ and expressed as:

$$Q_{SC} = \frac{S\sigma x}{d_0 + x} \tag{5}$$

Eq. 2 is derived from an electronic perspective of a vertical contact-separation TENG, i.e., an equivalent circuit model composed of a voltage source that is identical to the potential induced by the electrostatic surface charge, i.e., the open-circuit voltage of TENG V_{OC}, and an inherent capacitor with a variable capacitance C_{TENG} connected in series [34]. This model is illustrated in Fig. 4(a), with the expression of V_{OC} and C_{TENG} presented by Eq. 3 and Eq. 4 respectively. Besides, the waveform of V_{OC} and C_{TENG} is illustrated in Fig. 4(c) when TENG operates in sinusoidal vibration. It is advantageous in its direct relationship with the physical mechanism of TENG, as well as the linearity between the V_{OC} and x.

According to Norton's theorem, this model can be transformed into a current source, which is identical to the short-circuit output current I_{SC}, in parallel with the internal impedance, as presented in Fig. 4(b). Due to the time-varying capacitance C_{TENG}, the expression of I_{SC} with respect to the displacement of TENG will be complicated. Nevertheless, this model is advantageous in analyzing the phase difference between the output voltage and current, and thus is commonly utilized in active energy extractor design.

One problem with the V-Q-x relationship of the TENG shown in Eq. 1 is that this equation is not always valid when x approaches or exceeds the width of the dielectric. In that case, the electric field becomes nonuniform, and the induced potential becomes nonlinear to x [32]. In practice, when x exceeds a certain threshold, the increase of V_{OC} cannot match the decrease of C_{TENG}; hence the voltage across the TENG will drop, or invert if the TENG is in a loop. The specific relationship between V_{OC} and x under this condition is complicated and influenced by many factors, such as the shape and width of the dielectric, etc. In practice, this situation can be avoided with several methods. The first method is to assume that the V_{OC} stays unchanged when x exceeds a certain threshold in simulations. This is the most convenient method but can be inaccurate and may lead to unexpected output, such as voltage drop or inversion. Another method is to limit the displacement of TENG in both simulation and practice. This solution guarantees consistency between simulation and experiment but is not always practical.

Then, the V-Q-x relationship of lateral-sliding TENG will be introduced. The freestanding TENG has a similar property to the lateral-sliding TENG so they share the same relationship. Despite different motion modes, the Eq. 2 is still valid in this mode, which means that the equivalent circuit models presented in Fig. 4 also work in lateral-sliding TENG. However, the parameters C_{TENG} and V_{OC} of it as well as Q_{SC} are different from those of vertical contact-separation TENG aforementioned, which are supposed to be

$$C_{TENG} = \frac{\epsilon_0 w(l - x)}{d_0} \qquad (d_0 = \frac{d_1}{\epsilon_{r1}} + \frac{d_2}{\epsilon_{r2}}) \tag{6}$$

$$V_{OC} = \frac{\sigma x}{\epsilon_0 (l - x)} d_0 \tag{7}$$

$$Q_{SC} = \sigma w x \tag{8}$$

where l and w denote the length and width of the plate respectively. All symbols represent the same parameters as those in the contact-separation TENG and are labeled in the theoretical model illustrated in Fig. 3b [33]. These equations are valid when x is smaller than l. When x is larger than l, the V_{OC} is not related to the displacement but only determined by the electrostatic surface charge induced by the triboelectric effect. In lateral-sliding and freestanding TENGs, the I_{SC} of the current source model is linear to the x. However, as it is still not always equal to the current from the source, the voltage source model is recommended in lateral-sliding TENGs as well.

Inspired by the V-Q-x relationship, the V-Q plot has been utilized to analyze the TENG output [35]. An example of the V-Q plot is illustrated in Fig. 5. The V axis represents the voltage across the TENG, while the Q axis represents the output charge. V_{OC+} is identical to V_{OC} at the maximum displacement, and the Q_{SC+} is the total charge output on that

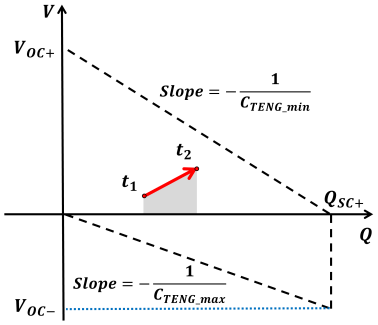

Fig. 5. The V-Q plot of TENG.

condition. V_{OC-} is identical to the voltage across the internal capacitor when the charge on that is equal to Q_{SC+} and the capacitance C_{TENG} reaches the maximum. In this case, the slope of the dashed lines connecting $(0, V_{OC+})$ and $(Q_{SC+}, 0)$ is the reciprocal of the minimal C_{TENG}, while that connecting origin and the point (Q_{SC+}, V_{OC-}) is the reciprocal of the maximal C_{TENG} as presented in Fig. 5. The output energy can be calculated by the following equation:

$$E = \int VIdt = \int VdQ \tag{9}$$

Eq. 9 indicates that the output energy can be conveniently represented by an area in the V-Q plot. As illustrated in Fig. 5, when TENG works from t_1 to t_2, the energy output is represented by the shadow area and thus can be calculated mathematically. Therefore, the V-Q plot is useful in triboelectric energy harvesting design to calculate energy extraction performance.

B. Requirements for Extracting Triboelectric Energy

Based on the characteristics of TENG analyzed before, some requirements for triboelectric energy harvesting can be summarized. First, if a TENG is experiencing a periodic mechanical motion, the output of the TENG is an alternating-current (AC) energy due to the internal capacitor. To use the harvested energy and power load electronics, the AC energy needs to be converted to the direct-current (DC) form with a rectification technique. Unlike the piezoelectric and electrostatic transducers, the TENG is not typically implemented in vibration environments, making its output similar to a shock in a mono-directional motion cycle [36], [37]. Additionally, the voltage and current outputs are usually asymmetric for motion in different directions, even with the same distance [36], [38]. Therefore, those rectifiers applied in triboelectric energy harvesting should work with fast-changing input.

Another problem caused by the internal capacitor is that it will generate a phase difference between current and voltage outputs when the TENG is loaded capacitively. In this case, an amount of charge will be wasted to compensate for the phase delay of voltage; as a result, the energy extraction performance is degraded. In piezoelectric energy harvesting, some mature solutions to eliminate that phase difference have been proposed and employed, such as the synchronous switching techniques including synchronous electric charge extraction (SECE) technique [39] and synchronized-switch harvesting on inductor (SSHI) technique [40]. However, different from the constant internal capacitance of the piezoelectric transducer, the internal capacitance of TENG is time-varying, which limits the effectiveness of those techniques.

Besides, the internal impedance of TENG is very high due to the small internal capacitance and low operating frequency. In practice, this causes high output voltage when TENG is loaded with high resistance or in open-circuit conditions, where high voltage tolerance of devices in the interfaces is typically required. On the other hand, if the load impedance is small, the current can rocket sharply at the beginning but drop soon, and in this case, the power output is very low [41]. Therefore, to extract more energy from a TENG, the power management interface must optimize its load impedance or the rectification voltage based on the time-varying internal impedance of the transducer [42].

In summary, the internal time-varying capacitive impedance makes triboelectric energy harvesting much different from the energy harvesting of other mechanical energy harvesters. Over the past decade, several techniques were reported to extract more energy from TENG. Commonly, the viability and performance of an energy harvesting interface can be evaluated from the following perspectives: (1) Efficiency; (2) Stand-alone operation; (3) Circuit complexity; (4) Adaptivity; (5) Microscale compatibility [43]. Therefore, those energy harvesting techniques are evaluated from these perspectives and reviewed in the following sections.

III. Passive Converters

Among all power conversion techniques, passive power converters are widely employed due to their simplicity, stability, and capability for a cold startup, though they typically suffer from low energy conversion efficiency. Passive converters are composed of passive components such as capacitors, diodes, or diode-connected transistors. The most typical passive converter is the bridge rectifier, which can be divided into two types: half-bridge rectifier (HBR) and full-bridge rectifier (FBR). Besides, rectification can be implemented together with voltage regulation via switched-capacitor technologies. Two passive switched-capacitor converters, voltage multiplier and Bennet's doubler of electricity, have been reported in harvesting triboelectric and electrostatic energy as well as other power management systems. These AC-DC converters will be introduced respectively, with their feasibility, strengths, and weaknesses in triboelectric energy harvesting applications.

A. Passive Bridge Rectifiers

Full bridge and half bridge are the two most common configurations of rectifiers. The half-bridge rectifier comprises two diodes, where one diode allows current in one direction to pass while the other diode shorts the AC source. The full-bridge rectifier (FBR) employs two half-bridge rectifiers to regulate the current in both polarities. This topology can rectify current regardless of its polarity, allowing it to extract more energy than the half-bridge configuration in one cycle; hence, it has been implemented in most harvesters. The energy harvesting interface comprising an FBR and a rectification capacitor is named a standard energy harvesting circuit, as presented in Fig. 6a. When the rectification voltage,

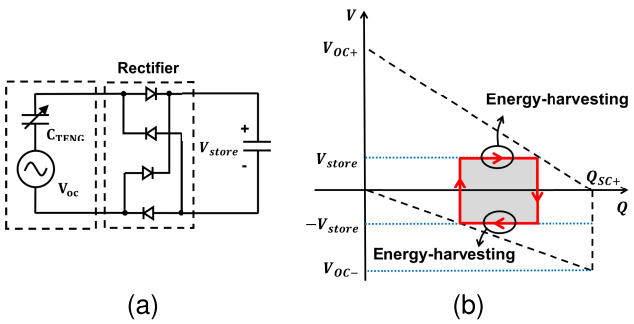

Fig. 6. (a) The configuration and (b) V-Q plot of the standard energy harvesting circuit in triboelectric energy harvesting.

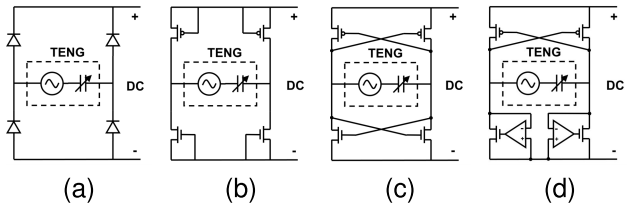

Fig. 7. Different configurations of full-bridge rectifiers in triboelectric energy harvesting. (a) Passive diode rectifier; (b) Diode-connected gated rectifier; (c) Cross-coupled rectifier; (d) Active-diode rectifier [46].

i.e., the storage voltage V_{store} in this case, is fixed, the V-Q plot of a standard energy harvesting circuit in triboelectric energy harvesting is illustrated in Fig. 6b. The shaded area indicates the energy output per cycle, which is determined by the output charges and the rectification voltage.

In practice, implementing an FBR in triboelectric energy harvesting faces several challenges, which differ regarding application scenarios. For instance, in low-power applications, the input voltage is low, so the rectifier should emphasize the suppression of the leakage current and conduction loss, while in high-power applications, it must tolerate high rectification voltage, but the voltage drop on the diode is comparatively negligible. Therefore, the implementations of FBR in low-voltage and high-voltage applications will be discussed separately in the following part.

1) Low-Voltage Full-Bridge Rectifiers: A significant application of triboelectric nanogenerator (TENG) is to harvest kinetic energy from human motion and power some lightweight wearable devices. In this case, TENG usually has nano-Watts output due to its small size and low working frequency. Due to the high internal impedance, it outputs several volts with nanoampere-level alternating current. The advantage is that the system can start working from a cold state easily. However, the power consumption and leakage of the harvester must be very low. The integrated FBR is more suitable in this situation with low leakage, smaller size, and lower price compared to the discrete rectifier. For on-chip implementation, the ordinary PN-junction-based diode, presented in Fig. 7a, cannot be directly applied, which has a high risk of latch-up, so the gated diode rectifier is proposed with the diode-connected transistors as presented in Fig. 7b [44]. This is the simplest way to implement an integrated FBR, but it has several drawbacks. First, the power conversion efficiency of this design in low-voltage systems is restricted by the forward voltage drop of diode-connected transistors [45]. Besides, the weak inversion leakage of transistors can be fatal in low-power energy harvesting systems.

To decrease the conduction loss caused by transistors, a different configuration that used to be widely employed in piezoelectric energy harvesting can be employed, which is the cross-coupled rectifier, i.e., negative voltage converter [46]. It is illustrated in Fig. 7c. In this topology, the voltage drop is suppressed considerably, but the reflux current of this rectifier may be bothering when the input voltage is lower than the output voltage [45]. Another configuration is the active-diode topology illustrated in Fig. 7d, where one pair of NMOS in the cross-coupled rectifier is replaced by transistors gated by comparators. Since the comparator can amplify the voltage difference between the input and output, the conduction loss on the transistors is suppressed and the current permittivity is raised. However, this rectifier relies on a voltage supply to power the amplifiers [47].

Regarding the leakage loss, the active-diode rectifier can block the leakage current but the cross-coupled rectifier can make it worse. One possible amelioration to it is to cascade multiple cross-coupled pairs [48], [49]. Another solution is to substitute the cross-coupled CMOS pair to each transistor [50]. It is composed of a PMOS and an NMOS gated by the source of each other, which guarantees an off-voltage further from 0 and thus eliminates leakage current. A dynamic leakage suppression rectifier is implemented in [51] with four cross-coupled CMOS pairs and employed to harvest electrical energy from a low-power TENG. The leakage suppression of it is demonstrated effective.

2) High-Voltage Full-Bridge Rectifiers: Despite application scenarios in the low-voltage domain, TENG is also promising in high-power energy harvesting. For instance, a 12.6 cm^2 TENG can output 1.2 mW power [52]. However, due to the high internal impedance of TENG, high power density is always accompanied by high voltage, so the diodes must tolerate high reverse voltage in this case. Since some discrete diodes can easily tolerate a voltage as high as thousands of volts, most triboelectric energy harvesting circuits reported so far are designed with discrete components [53], [54]. However, external rectifiers implemented with commercial or self-designed diodes are not cost-friendly in terms of the printed circuit board (PCB) area compared to integrated circuit (IC) [55]. Besides, active energy extraction techniques can be implemented and enclosed in the power management unit, which boosts the efficiency and decreases cost and size. Therefore, the integrated high-voltage rectifier for TENG was being explored.

A typical high-voltage IC technique is based on the high-voltage bipolar-CMOS-DMOS (BCD) technology. The most cost-friendly choice by now is the high-performance power lateral double-diffused MOS (LDMOS). It is constructed with an internal PN-junction with a breakdown voltage of up to 70V [56]. Besides, the new generation of high-voltage semiconductors including Silicon Carbide (SiC) and Gallium Nitride (GaN) is expected to improve the triboelectric energy harvesting efficiency in the future.

Based on these high-voltage IC techniques, some power conditioning techniques implemented on chips are promising to tackle the constraints introduced in Section II-B, including the asymmetric and fast-changing output of TENG and

the polarity difference between voltage and current, with negligible power consumption compared to the extra energy harvested from TENG. For instance, an integrated high-voltage dual-output rectifier (DOR) is reported to make full use of the asymmetric output of TENG [57]. The conventional full-bridge rectifier (FBR) has a single output terminal, while in this work, it is split into two. Besides, the instantaneous voltage drop of TENG caused by the nonlinearity of the potential field is also taken into consideration. To extract more energy in this case, the rectification voltages at different output terminals are set differently. This also eliminates part of the phase difference and consequently extracts more charge from TENG. In the implementation, a high voltage protector is designed to avoid the current leakage between the outputs of DOR [55]. This architecture can be improved in topology by isolating the outputs with the inductor to remove the protector and suppress the power dissipation of the interface circuit [58], [59].

Nevertheless, the polarity difference of the TENG output cannot be entirely eliminated by FBR so different topologies are expected. In [60], it is reported that the charge extracted by the half-bridge rectifier per cycle exceeds that of FBR when the rectification voltage goes higher. This is because the half-bridge rectifier shorts the TENG periodically, which eliminates the phase difference caused by the internal capacitor. Consequently, the passive half-bridge rectifier might be a solution to this problem but it wastes much energy in the short-circuit phase [61]. This problem also occurs in piezoelectric and electrostatic energy harvesting, where some mature solutions have been proposed that can contribute to triboelectric energy harvesting. Those techniques will be reviewed in Section IV.

B. Passive Switched-Capacitor Converters

Though bridge rectifiers are highly effective and efficient in rectification, they cannot regulate the output voltage. Hence a DC-DC regulator has to be additionally added to the harvesters after the bridge rectifier. If the rectification and regulation can be integrated into one converter, the end-to-end efficiency of energy harvesting is expected to be improved. Such an AC-DC converter can be implemented with capacitors and passive diodes, named a passive switched-capacitor converter. It does not need external control signal to drive the voltage conversion but utilizes the inherent polarity switching of AC input, thus the implementation of passive switched-capacitor converters is simplified. However, this makes the conversion speed and efficiency dependent on the AC input frequency and thus it is usually employed in high-frequency AC energy harvesting. Besides, due to a large number of passive diodes in the converter, the conversion loss is significant. To improve the conversion performance, the passive diodes can be replaced by active switches controlled by comparing the AC input to suppress the conduction loss [62].

In the following part, two typical passive switched-capacitor converters used in energy harvesting will be introduced respectively based on the ascend and descend of voltage outcome: voltage multiplier and Bennet's doubler of electricity.

1) Voltage Multiplier: A voltage multiplier is a typical passive switched-capacitor converter usually used in a step-up circuit [64]. Two commonly used configurations of it are illustrated in Fig. 8, which are the Cockcroft-Walton configuration and Karthaus-Fischer configuration respectively [63]. It can commutate the current and regulate the voltage outcome to multiple times the magnitude of the energy source V_{in} autonomously based on the number of diode-capacitor pairs. As the voltage output of triboelectric nanogenerator (TENG) is inherently high, an ultra-high voltage can be gained by the voltage multiplier, which is required by certain devices e.g., AC electroluminescence device [65]. However, this converter is not suitable to regulate TENG for powering the microsystem that requires a low voltage supply.

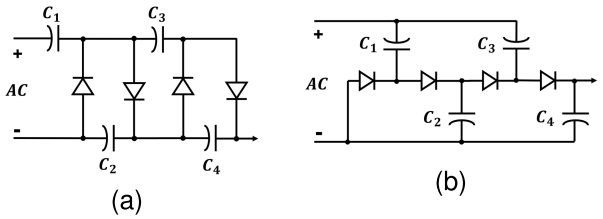

Fig. 8. Passive voltage multiplier in (a) the Cockcroft-Walton configuration, and (b) the Karthaus-Fischer configuration [63].

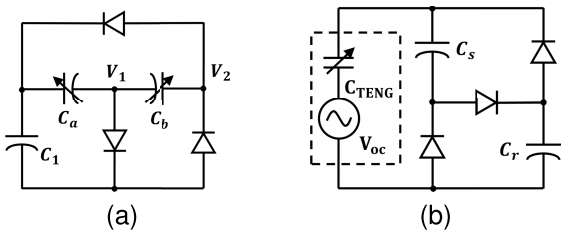

Fig. 9. Bennet's charge doubler in (a) electrostatic voltage conditioning [66] and (b) triboelectric voltage conditioning [67].

2) Bennet's Doubler of Electricity: Bennet's doubler of electricity was first proposed hundreds of years ago and was designed to induce and extract extra charge by shifting the capacitance at the beginning [68]. Its application in charging storage elements is illustrated in Fig. 9a [66]. For each working cycle, the variable capacitor C_a shrinks its capacitance first to decrease the voltage V_1 and induce charges on the other variable capacitor C_b. Then C_a resets while C_b decreases its capacitance to increase the voltage V_2 so that extra charges are pumped back to the storage element C_1. At the end of each cycle, the charge on C_1 increases, and so is the energy. This technique has been used in electrostatic energy harvesting as these variable capacitors are identical to the electrostatic pumps of electrostatic generators [69], [70], [71], [72]. Since the internal capacitor of TENG is also variable, the implementation of Bennet's doubler in triboelectric energy harvesting is explored.

The first application of Bennet's doubler in triboelectric energy harvesting is proposed by [67] with the structure presented in Fig. 9b. To extract charge from TENG and decrease the output voltage meanwhile, this structure is different from the prior Bennet's doubler and utilizes two static capacitors C_s and C_r to halve the output voltage. In each cycle, C_s and C_r extract charges from TENG in series when its internal capacitance C_{TENG} is small, and transfer more charges back in parallel when C_{TENG} is large. There are two operation modes determined by the ratio between the maximum and the minimum of C_{TENG}, which is denoted as μ. When $\mu > 2$, Bennet's doubler works in the exponential mode

that the output voltage diverges and increases exponentially. When $\mu < 2$, the voltage will increase convergently and saturate after a certain number of cycles [67]. Commonly, C_{TENG} varies significantly, so Bennet's doubler usually works in the exponential mode in triboelectric energy harvesting. In this case, the charge extracted to C_s and C_r per cycle will increase exponentially, as well as the power output; hence the energy extracted by Bennet's doubler can easily exceed that of the passive full-bridge rectifier, where the charge output decreases when the rectification voltage increases. In addition, the energy gained by Bennet's doubler concentrates on the capacitor with the largest capacitance among C_{TENG}, C_s, and C_r, which makes it easy to be harvested [67]. These strengths make Bennet's doubler a very promising approach to triboelectric energy harvesting, having been employed in several works [73], [74], [75].

However, there are several drawbacks limiting the application of Bennet's doubler in triboelectric energy harvesting. The first one is the long warm-up time of Bennet's doubler at the first use. Despite the exponential boosting of the charge accumulated on the capacitor, the charge induced per cycle at the beginning is very small, so it takes multiple cycles to reach the proposed operational voltage based on the working frequency of TENG [76]. Additionally, the output voltage of Bennet's doubler fluctuates, resulting in extra energy loss, and thus, an extra voltage stabilization technique is required to provide a steady voltage supply.

IV. Active Converters

Active converters are implemented with active switches that have lower conversion loss compared to passive devices. Though additional gate drivers and control circuits are required, some actively-switching converters can tackle the aforementioned polarity difference between voltage and current outputs of TENG, which significantly increases the power output by multiple times that of a standard energy harvesting circuit.

This section introduces two synchronous-switching techniques: synchronous electric charge extraction (SECE) and synchronized-switch harvesting. Both have been widely applied in piezoelectric energy harvesting to avoid the efficiency degradation caused by the polarity difference. In addition, the active switched-capacitor converter will also be discussed, which can be fully integrated and thus benefits from smaller size and processing advance.

A. Synchronous Electric Charge Extraction (SECE)

SECE is a popular active rectification technique to boost energy extraction performance and was first designed for piezoelectric energy harvesting [39]. The typical circuit and voltage waveform is illustrated in Fig. 10a and Fig. 10b, respectively. Unlike the standard energy harvesting circuit, the rectifier is directly connected to the voltage regulator without a rectification capacitor. For most time in each semi-period, the transducer is isolated, so the output voltage is identical to the open-circuit voltage. When the voltage reaches an extremum, the inductor extracts the energy rapidly through the red path in phase 1 (ϕ_1), as presented in Fig. 10a. Since all charges accumulated on the internal capacitor are extracted, the voltage is reset at the end of ϕ_1, so there is no polarity difference between current and voltage output. Then the source is again isolated in the next semi-period when the energy temporarily stored in the inductor is transferred to the storage element C_{store} through the blue path in phase 2 (ϕ_2) [77]. In this way, the energy output is enhanced compared to the standard energy harvesting circuit because the charge is extracted and harvested at a higher voltage. Note that the quadra-switch design realizes a buck-boost regulator, so theoretically, the output of SECE can be directly used to power electronic devices.

The energy output of TENG enhanced by SECE is analyzed and presented by the V-Q plot in Fig. 10c. Due to the open-circuit phase in SECE, the charge is extracted from TENG at V_{OC} so the energy output is boosted. The shaded area presents the theoretical extra energy output in each cycle compared to the standard energy harvesting circuit, which is considerable and verified in discrete circuits [78], [79].

Due to the high open-circuit voltage of TENG, most implementations of SECE in extracting triboelectric energy are discrete circuits with mechanical switches. Some switches utilize the structure of TENG and turn on autonomously when the electrode moves to the extremum [80], [81]. However, this design requires the electrode to move regularly so it is incompatible in different scenarios. To implement a fully-automatical and adaptive SECE harvester, IC technology is required. The current and voltage detector implemented by CMOS technology with a high-voltage integrated interface can be helpful in the application of SECE in harvesting triboelectric energy. A multi-shot energy extraction technique implemented on-chip has been proposed recently, utilizing SECE in limited voltage tolerance [82].

B. Synchronized-Switch Harvesting

The synchronized-switch harvesting technique is specialized to eliminate the polarity difference between voltage and current outputs to extract more energy. Its simplest topology comprises a full-bridge rectifier (FBR) and a switch placed across the energy source. The switch is turned on when the direction of the current shifts to remove the residual charge and reset the voltage. Thus it is named synchronous short-circuit rectifier (SSCR). It has been proven to be effective in synchronizing the voltage and current when TENG moves to the extremum [83]. Besides, this synchronous short-circuit path was recently added to the SECE interface in piezoelectric energy harvesting to ensure stability and increase the harvestable energy bandwidth [84], [85].

However, a large part of the energy accumulated on the internal capacitor is wasted by SSCR in short-circuit phase. This can be improved by utilizing an inductor to flip the voltage instead of resetting it, which is the synchronized-switch harvesting on inductor (SSHI) technique, i.e., bias-flip rectifiers. Based on different topologies of inductor connection, it can be divided into two types: parallel-SSHI and series-SSHI [86]. The typical parallel-SSHI circuit and operation waveform is illustrated in Fig. 11a and Fig. 11b, respectively. When the current direction shifts, the switch will be turned on so the voltage of the source, which was equal to the rectification voltage, is flipped by the inductor [87]. When the current in the inductor is zero, the voltage-flipping phase

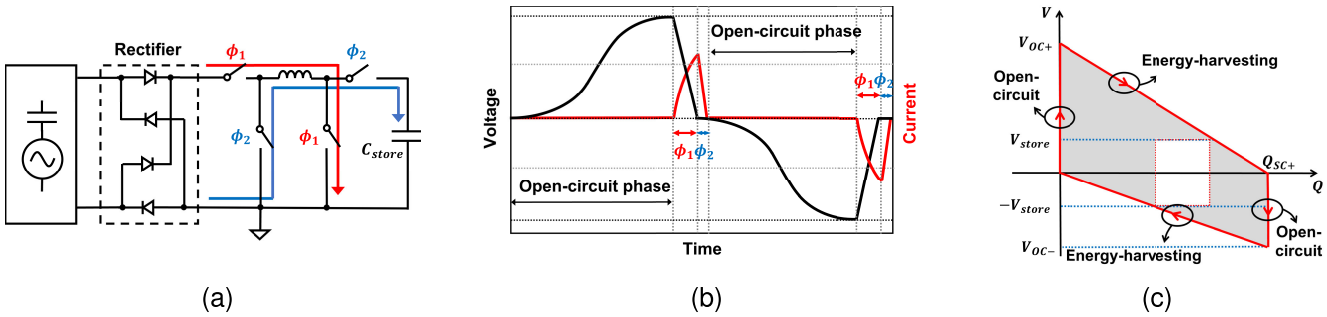

Fig. 10. (a) Schematic of a SECE interface connected to TENG with (b) operation voltage and current waveform and (c) V-Q plot of TENG.

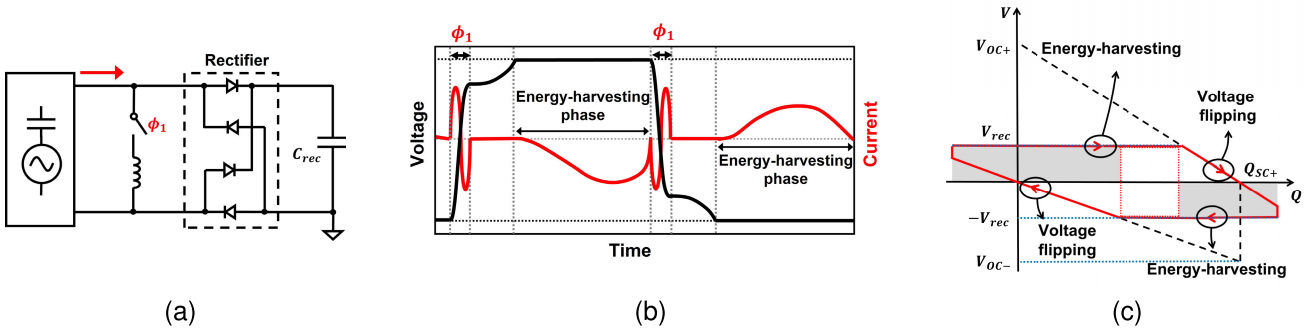

Fig. 11. (a) Schematic of a parallel-SSHI interface connected to TENG with (b) operation voltage and current waveform and (c) V-Q plot of TENG.

ϕ_1 ends so the switch is turned off. Due to the nonideality of the inductor, the voltage across the internal capacitor cannot be completely flipped so it needs to be charged to the rectification voltage before the current is harvested. Nevertheless, parallel-SSHI saves much energy from discharging the internal capacitor of the source and contributes to efficiency-boosting, especially when the rectification voltage is high. Series-SSHI has two ways of implementation. The first one has a similar phenomenon to that of parallel-SSHI but flips voltage via the shorted bridge rectifier rather than an independent path [88]. The other kind of series-SSHI is closer to SECE, with the bridge rectifier cut-off for most of the time and the energy extracted at the same time as voltage flipping [89], [90].

SSHI rectifiers can also be implemented in triboelectric energy harvesting. The V-Q plot of TENG with a parallel-SSHI interface is presented in Fig. 11c. The shadowed area in Fig. 11c is the extra energy harvested by the parallel-SSHI rectifier compared to the standard energy harvesting circuit. The parallel-SSHI is first implemented in triboelectric energy harvesting in a discrete circuit by [91]. Then the first integrated parallel-SSHI triboelectric energy harvesting circuit was implemented in [92] with an inductive step-down converter and a switched-capacitor DC-DC converter in series for voltage conditioning. In addition, thanks to the LDMOS, series-SSHI is more feasible since a short-circuit loop can be easily established within FBR. A double-stacked-chip series-SSHI employing an intrinsic fractal switched-capacitor converter (FSCC) is reported in [93] and [52]. It boosts energy harvesting by doubling the voltage tolerance of the harvester via two series-connected FBRs and storage capacitors on two stacked chips. When the current output is 0, both FBRs will be shorted to flip the voltage across TENG. This active converter is driven by an external power source, which is also the storage element. Another series-SSHI triboelectric energy harvester is reported in [94].

Despite the advantages of the SSHI technique, it is not fully integrated due to the off-chip inductor. Inductor also brings other problems, such as difficult control of flipping time and varying inductance, which lead to conversion loss [95], [96]. In this case, an inductor-less bias-flip rectifier was explored and implemented by the switched-capacitor technique called synchronized switch harvesting on capacitors (SSHC) [97], [98]. To achieve higher efficiency, multiple capacitors are necessary to flip the voltage smoothly to reduce the charge-sharing loss, which can be implemented with more parallel stages [99] or phase-split configuration [98]. This SSHC converter can be fully integrated. However, considering the variable capacitance C_{TENG}, the conventional SSHC circuit achieves lower efficiency in triboelectric energy harvesting than in piezoelectric energy harvesting so it needs to be redesigned before being applied.

C. Active Switched-Capacitor Converters

The aforementioned synchronous charge extraction and synchronized-switch harvesting techniques extract more energy from TENG but cannot regulate the voltage output; thus, a DC-DC converter should follow to condition the voltage. The most popular DC-DC converter is the inductive switching converter which is advantageous in wide conversion range, high efficiency, and high driving capacity. However, the inductor is relatively huge and cannot be integrated on-chip. Comparatively, the switched-capacitor converter (SCC) can regulate voltage with the converter fully integrated, which brings benefits in scalability.

The configurations of active SCCs are various. One common configuration is the fractal switched-capacitor converter (FSCC) [100]. A typical two-to-one FSCC is illustrated in Fig. 12a with the current flow in different working phases indicated. In this case, the output voltage is theoretically half

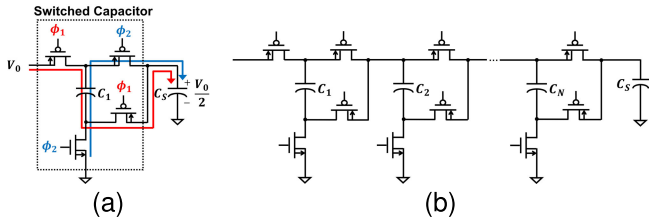

Fig. 12. (a) A typical 2-to-1 fractal switched-capacitor converter and (b) a reconfigurable switched-capacitor converter.

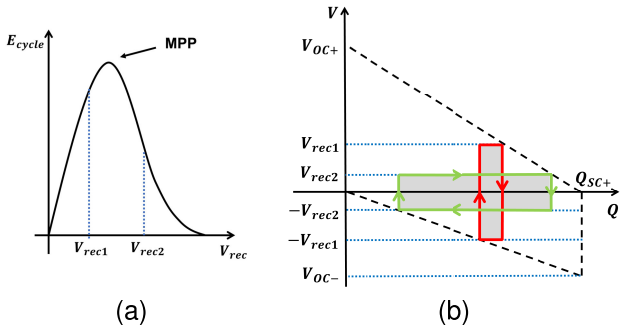

Fig. 13. (a) Typical pattern of output energy per cycle versus rectification voltage. (b) V-Q plot of MPPT in triboelectric energy harvesting.

of the input voltage. The conversion ratio can be changed with more switched-capacitor pairs but is fixed when the configuration of the converter is determined. The efficiency of SCC will degrade when the real voltage conversion ratio is different from the one determined by the configuration. In practice, the output voltage or input voltage usually varies; thus, it is usually hybridized with an inductive switching converter [92] or implemented in a reconfigurable topology, which is composed of multiple switched capacitors as illustrated in Fig. 12b but only part of them will be enables to achieve various conversion ratio [93], [94], [101].

Some active switched-capacitor converters are reported to harvest energy from high-voltage TENG, but all have severe weaknesses. [102] implemented it with mechanical switches, which can have connecting issues. Reference [103] reports a high-conversion-ratio regulator by replacing the switches with passive diodes to improve the voltage tolerance. Though the voltage output is degraded, the driving capacity of this converter is limited due to the low vibration frequency of TENG. Hence, a more efficient way of utilizing the integrated switched capacitor in high-voltage TENG needs to be explored.

V. Energy Harvesting Enhancing Techniques

The performance of triboelectric energy harvesting can be enhanced from different perspectives, including efficiency, independence, and costs. For instance, the aforementioned active converters improve energy extraction efficiency, while the IC technology lowers the cost and volume of the harvester. In this section, some other techniques contributing to better energy harvesting from TENG will be introduced. The maximum power point tracking (MPPT) technique is widely used in photovoltaic energy harvesting systems to guarantee that the transducer always produces the highest power output. Self-excitation explores the possible energy-boosting of cascaded electrostatic generators or TENGs. Cold-startup is a significant function of all self-sustained energy harvesting systems to eliminate the external power supply and, thus, improve compatibility and widen the application scenarios. With these techniques, triboelectric energy harvesting can be more applicable in real-world implementations.

A. Maximum Power Point Tracking

The power output is proportional to the real-time product of the voltage and current output of the energy source. The condition under which the system has the maximum power output is defined as the maximum power point (MPP) as illustrated in Fig. 13a, and the technique to track and maintain the voltage at the maximum power point is named maximum power point tracking (MPPT) and it plays an important role in energy harvesting systems. If the energy extracted from the transducer is consumed directly by a load, the maximum power point is reached when the load impedance is equal to the internal impedance of the energy source [104]. Since the impedance of TENG is time-varying, an active impedance matching method was studied in [105] to track it with a negative impedance converter model. On the other hand, impedance matching is not feasible when the energy is to be harvested and stored, but the voltage across the storage element is to be controlled. For instance, in a standard energy harvesting circuit, the maximal power output is tracked by monitoring the rectification voltage on the storage element since the charge output in one cycle usually is relative to the rectification voltage.

There are several methods to implement MPPT, including perturb and observe (P&O), incremental conductance (IncCond), and fractional open-circuit voltage (FOCV). Both P&O and IncCond track the maximum power point continuously by adjusting the rectification voltage and monitoring the difference in power output, i.e., the energy change stored in the load capacitor [106]. These two techniques are accurate but complicated to implement. On the other hand, the FOCV methodology is much simpler to be implemented. For many transducers, including piezoelectric transducers, electrostatic transducers, and triboelectric nanogenerators (TENG), the maximal power output usually occurs around a certain voltage with a fixed ratio to the open-circuit voltage [107]. Indeed, the V-Q plot that reflects the energy output of each cycle can contribute to virtually seeking the maximum power point of TENG, as presented in Fig. 13b. The red and green rectangles indicate the standard energy harvesting circuit working at different rectification voltages V_{rec1} and V_{rec2} respectively, while their areas represent the corresponding energy output. MPPT technique should track the rectification voltage when the energy output reaches the maximum, i.e., the maximum rectangle enclosed by the dashed lines. When the properties of TENG are fixed, the maximum power point can be quickly figured out mathematically, which is

$$V_{rec,mppt} = \frac{1}{2}\frac{V_{OC-}V_{OC+}}{V_{OC-} + V_{OC+}} \tag{10}$$

where V_{OC-} and V_{OC+} represent the asymmetric open-circuit voltage of TENG. By monitoring these two voltages and maintaining the rectification voltage at the $V_{rec,mppt}$, MPPT

TABLE I
COMPARISON TABLE OF THE STATE-OF-THE-ART

Rectifier	Passive converters					Active converters				
	FBR			Bennet's doubler		SECE	P-SSHI	S-SSHI		SSHCI
Reference	[115]	[55]	[59]	[67]	[73]	[82]*	[92]	[52]	[94]	[116]
Transducer	CS TENG	CS TENG	CS TENG	CS TENG	CS TENG	CS TENG	CS TENG	Wind TENG	Wind TENG	PT
Process	65 nm CMOS	0.18 um BCD	0.18 um BCD	Discrete	Discrete	0.18 um BCD	0.18 um BCD	0.18 um BCD	0.18 um BCD	0.18 um BCD
Modification	-	Dual-output rectifier	Dual-output rectifier	-	-	Multi-shot SCE	-	MCS-BF	-	-
Regulation	SCC	Dual-input BUCK	Dual-input BUCK	-	BUCK	BUCK-BOOST	BUCK +SCC	SCC	SCC	BUCK
MPPT	-	FOCV	FOCV	-	-	-	-	-	-	FOCV
$V_{EXT}(V)$	2.5	3.5 - 70	<70	835	450*	<70	12-70	$65 \times N$	<65	<5
PCE	88%	52.9%	75.6%	-	31.60%	63.28%	32.7%	70.7%	79.3%	83%
Output voltage	1.2	2 - 5	2.8 - 3.3	-	17	2 - 20	2	3.1 - 4.3	2.7 - 4.2	1.6 - 4.6*
$P_{EXT}(\mu W)$	2.4 - 15.6	4.5 - 20.9	3.9 - 10.5	70*	152	90.3	2.95	1200	300	29.2
FoM (nJ/cm^2)	-	80	64	140*	840	-	44	380	95	20
P_{EXT}/P_{FBR}	-	-	-	21×	7.7×	1.91×	1.62×	3.14×	-	5.44×

* Simulated results. ** Estimated.

can be implemented with less energy loss and a simpler control system. Due to its simplicity and relatively-high accuracy, the FOCV technique is implemented in the integrated dual-output rectifier (DOR) reported in [57] and [59]. In this work, it is taken into account the different maximum power points of TENG at different phases, so they implement separate FOCV MPPT for either output of DOR.

MPPT technique can also be utilized to maintain the maximal power output in active converters, where impedance matching and storage voltage optimization are also required [108]. So far, it has not been integrated into active triboelectric energy harvesting. In both SECE and SSHI interface, the maximum power point is determined by two parameters: the maximal open-circuit voltage of TENG and the nonideality of the inductor [109]. Both parameters may vary in practice, making tracking the maximal power output difficult. Besides, the rectification voltage at the maximum power point can be multiple times the open-circuit voltage of TENG, which can hardly be measured by integrated circuit [110]. Further research is needed to solve these obstacles.

B. Self-Excitation

In some works, the energy output of TENG is strengthened by extra charge provided by external energy sources such as batteries or another TENG, which is called the self-excitation technique [111], [112], [113]. Those sources or storage elements charge TENG at low voltage and harvest electrostatic energy at high voltage. This methodology is advantageous in boosting the charge density on TENG without changes in the triboelectrification of the material. However, it still needs caution about the internal breakdown of TENG caused by the high voltage across it. Besides, accurate and automatic synchronization is required in the charge depositing and withdrawing.

C. Cold Startup

Active converters rely on steady power supplies to work. To build a battery-less system without an external power supply, the system must be capable of activating from the cold state. The cold startup technique has been widely employed in piezoelectric and electrostatic energy harvesting. Typically, it is implemented with a passive path that can rectify and harvest the energy, though with low efficiency, before the active parts in the system start operating. When the stored energy is high enough to drive the active converters and logic circuits, the active interface takes over the energy harvesting process to increase efficiency. Some self-driven triboelectric energy harvesting interfaces are reported, with the cold startup via discrete diodes [114] or integrated transistors [55].

VI. COMPARISON AND DISCUSSION

The state-of-the-art of triboelectric energy converters in the previous 5 years is summarized in Table. I. This table summarizes their process, conversion techniques, and performance and evaluates the circuit complexity and figure of merit (FoM). In triboelectric energy harvesting, the FoM is defined as the energy extracted from TENG per cycle with a normalized size. It is derived from the following equation:

$$FoM = \frac{P_{EXT}}{f_{OP} \times S} \tag{11}$$

where P_{EXT} represents the power extracted from TENG, i.e., the power input to the harvester, and f_{OP} represents the operational frequency. It depicts the absolute energy extraction capacity of the harvester while the fraction of P_{EXT} over the power extracted by FBR (P_{FBR}) only reflects the relative energy extraction capability. Therefore, a higher FoM corresponds to a higher energy extraction capacity of the harvester and better transduction performance of TENG. Besides, the voltage regulator employed in each work is

mentioned, as well as the relevant results, such as the power conversion efficiency (PCE) of the whole interface and the output voltage, which reflects their performance and compatibility.

Among the state-of-the-art, contact-separation TENG (CS TENG) is the most employed TENG due to easier fabrication and modeling. Wind TENG is also reported to be employed in harvester development. Unlike the aforementioned fundamental TENG, it has a fixed internal capacitance and works at a higher operational frequency identical to the vibration of triboelectric film driven by the airflow, so its energy extraction is relatively more straightforward [52], [94]. In addition, one case of piezoelectric energy harvesting is included to present the difference between energy extraction from TENG and piezoelectric transducer (PT).

In general, the harvesters implemented with passive devices such as FBR and Bennet's Doubler are simpler than those with active switches; however, they have low adaptivity and compatibility without voltage regulation implemented by active switches. IC technology is advantageous in implementing active converters in miniaturization and lower leakage but is limited in voltage tolerance. That is the reason why Bennet's Doubler implemented discretely has higher extraction capacity than integrated FBR, dual-output rectifier (DOR), synchronized-switch harvesting on inductor (SSHI), and synchronous charge extraction (SCE) based on the FoM. Among the IC works implemented with 65nm CMOS or 0.18um BCD process, their extraction voltage V_{EXT} are lower than 70V due to process limitation and thus achieves relatively lower FoM, except the work [52], which exceeds the voltage limitation via the multi-chip-stacked bias-flip (MCS-BF) technique. As a consequence, its FoM is more than 4 times higher than other IC works.

Furthermore, it is noted that few works in triboelectric energy harvesting employ MPPT. The reason is that most harvesters reach the maximum power point (MPP) when operating at the highest allowed voltage. In other words, the ideal MPP has exceeded the breakdown voltage of the device. In this case, the MPP of the triboelectric harvester can be easily tracked by operating it at the highest allowed voltage.

VII. Conclusion

A triboelectric nanogenerator (TENG) is a new mechanical energy transducer that performs high-efficiency energy harvesting from low-frequency and irregular mechanical motion; thus it has wide application scenarios, from biological motion energy harvesting to tide energy harvesting. Due to its different characteristics from those of prior transducers, specific energy harvesting interface circuits need to be designed to achieve high conversion efficiency. This work summarizes TENG energy harvesting requirements and recent advancements in triboelectric energy harvesting techniques. Due to the small and time-varying internal capacitance, TENG can generate asymmetric high-voltage output, which is one of the biggest obstacles in extracting energy harvested by TENGs. Fortunately, some mature methodologies employed in piezoelectric and electrostatic energy harvesting systems have been demonstrated feasible and advantageous in triboelectric energy harvesting. Passive converters take advantage of simplicity and, thus, are widely employed in triboelectric rectification. Active rectifiers such as synchronized electric charge extraction (SECE) rectifiers and synchronous switch harvesting rectifiers are effective in improving the performance of energy extraction from TENG by eliminating the phase difference between the voltage and current outputs. Besides, the switched-capacitor technique is advantageous in the CMOS process, thanks to the compatibility for on-chip integration and flexible voltage conditioning; as a result, it has been employed in triboelectric energy harvesting. An innovative switched-capacitor converter, Bennet's doubler of electricity, previously utilized to extract electrostatic energy from the capacitance varying, has been demonstrated to show promising performance in triboelectric energy harvesting. These conversion techniques are summarized in one table in this review, with their performance quantified.

Nevertheless, the state-of-the-art designs in triboelectric energy harvesting show relatively low efficiency and narrow application scenarios. One reason is that most energy harvesting techniques are borrowed from prior piezoelectric or electrostatic energy harvesting solutions. As TENGs have very different characteristics and voltage/current responses due to the varying internal capacitance, those techniques cannot fully explore the potentials of TENGs; therefore, specific design considerations and efforts are needed for TENG energy extraction techniques. Besides, triboelectric energy harvesting designs should also be specialized according to different applications, where the features of TENGs vary significantly. For future work, novel bias-flip and energy extraction topologies considering varying internal capacitance are needed. Interface circuits extracting energy from irregular mechanical movements are of great interest to broaden the applications scenarios of TENG energy harvesting systems. In addition, employing high-voltage devices to cope with the high TENG voltage is a promising approach to extracting more energy from TENGs. Furthermore, integrating TENGs into multiple-source energy harvesting systems will enable the autonomous systems to be fully sustained in fast-varying or harsh environmental conditions.

References

[1] Z. L. Wang, "On the first principle theory of nanogenerators from Maxwell's equations," *Nano Energy*, vol. 68, Feb. 2020, Art. no. 104272.

[2] F.-R. Fan, Z. Q. Tian, and Z. L. Wang, "Flexible triboelectric generator," *Nano Energy*, vol. 1, no. 2, pp. 328–334, 2012.

[3] T. Cheng, Q. Gao, and Z. L. Wang, "The current development and future outlook of triboelectric nanogenerators: A survey of literature," *Adv. Mater. Technol.*, vol. 4, no. 3, Mar. 2019, Art. no. 1800588.

[4] J. Luo and Z. L. Wang, "Recent advances in triboelectric nanogenerator based self-charging power systems," *Energy Storage Mater.*, vol. 23, pp. 617–628, Dec. 2019.

[5] C. Wu, A. C. Wang, W. Ding, H. Guo, and Z. L. Wang, "Triboelectric nanogenerator: A foundation of the energy for the new era," *Adv. Energy Mater.*, vol. 9, no. 1, pp. 1802906-1–1802906-25, 2019.

[6] Y. Wang, Y. Yang, and Z. L. Wang, "Triboelectric nanogenerators as flexible power sources," *NPJ Flexible Electron.*, vol. 1, no. 1, pp. 1–10, Nov. 2017.

[7] Z. L. Wang, T. Jiang, and L. Xu, "Toward the blue energy dream by triboelectric nanogenerator networks," *Nano Energy*, vol. 39, pp. 9–23, Sep. 2017.

[8] J. Zhao et al., "Remarkable merits of triboelectric nanogenerator than electromagnetic generator for harvesting small-amplitude mechanical energy," *Nano Energy*, vol. 61, pp. 111–118, Jul. 2019.

[9] Z. Wen et al., "Self-powered textile for wearable electronics by hybridizing fiber-shaped nanogenerators, solar cells, and supercapacitors," *Sci. Adv.*, vol. 2, no. 10, Oct. 2016, Art. no. e1600097.

[10] Y. Song et al., "High-efficiency self-charging smart bracelet for portable electronics," *Nano Energy*, vol. 55, pp. 29–36, Jan. 2019.

[11] K. Parida, J. Xiong, X. Zhou, and P. S. Lee, "Progress on triboelectric nanogenerator with stretchability, self-healability and bio-compatibility," *Nano Energy*, vol. 59, pp. 237–257, May 2019.

[12] S. Zhang, M. Bick, X. Xiao, G. Chen, A. Nashalian, and J. Chen, "Leveraging triboelectric nanogenerators for bioengineering," *Matter*, vol. 4, no. 3, pp. 845–887, Mar. 2021.

[13] Y. Su et al., "Self-powered room temperature NO_2 detection driven by triboelectric nanogenerator under UV illumination," *Nano Energy*, vol. 47, pp. 316–324, May 2018.

[14] Y. Song et al., "Wireless battery-free wearable sweat sensor powered by human motion," *Sci. Adv.*, vol. 6, no. 40, Oct. 2020, Art. no. eaay9842. [Online]. Available: https://www.ncbi.nlm.nih.gov/pubmed/32998888

[15] T. Tat, A. Libanori, C. Au, A. Yau, and J. Chen, "Advances in triboelectric nanogenerators for biomedical sensing," *Biosensors Bioelectron.*, vol. 171, Jan. 2021, Art. no. 112714.

[16] Q. Zheng et al., "In vivo powering of pacemaker by breathing-driven implanted triboelectric nanogenerator," *Adv. Mater.*, vol. 26, no. 33, pp. 5851–5856, 2014.

[17] Y. Fang et al., "Ambulatory cardiovascular monitoring via a machine-learning-assisted textile triboelectric sensor," *Adv. Mater.*, vol. 33, no. 41, Oct. 2021, Art. no. 2104178.

[18] Z. Li et al., "Elastic Cu@PPy sponge for hybrid device with energy conversion and storage," *Nano Energy*, vol. 58, pp. 852–861, Apr. 2019.

[19] Z. Li, Q. Zheng, Z. L. Wang, and Z. Li, "Nanogenerator-based self-powered sensors for wearable and implantable electronics," *Research*, vol. 2020, pp. 1–25, Jan. 2020.

[20] W. Ding, A. C. Wang, C. Wu, H. Guo, and Z. L. Wang, "Human–machine interfacing enabled by triboelectric nanogenerators and tribotronics," *Adv. Mater. Technol.*, vol. 4, no. 1, Jan. 2019, Art. no. 1800487.

[21] P. Tan et al., "A battery-like self-charge universal module for motional energy harvest," *Adv. Energy Mater.*, vol. 9, no. 36, Sep. 2019, Art. no. 1901875.

[22] J. Xue, Y. Zou, Y. Deng, and Z. Li, "Bioinspired sensor system for health care and human–machine interaction," *EcoMat*, vol. 4, no. 5, Sep. 2022, Art. no. e12209.

[23] X. Wang, S. Niu, Y. Yin, F. Yi, Z. You, and Z. L. Wang, "Triboelectric nanogenerator based on fully enclosed rolling spherical structure for harvesting low-frequency water wave energy," *Adv. Energy Mater.*, vol. 5, no. 24, Dec. 2015, Art. no. 1501467.

[24] Z. Lin et al., "Super-robust and frequency-multiplied triboelectric nanogenerator for efficient harvesting water and wind energy," *Nano Energy*, vol. 64, Oct. 2019, Art. no. 103908.

[25] B. Chen, Y. Yang, and Z. L. Wang, "Scavenging wind energy by triboelectric nanogenerators," *Adv. Energy Mater.*, vol. 8, no. 10, Apr. 2018, Art. no. 1702649.

[26] Z. Ren, L. Wu, Y. Pang, W. Zhang, and R. Yang, "Strategies for effectively harvesting wind energy based on triboelectric nanogenerators," *Nano Energy*, vol. 100, Sep. 2022, Art. no. 107522.

[27] R. D. I. G. Dharmasena and S. R. P. Silva, "Towards optimized triboelectric nanogenerators," *Nano Energy*, vol. 62, pp. 530–549, Aug. 2019.

[28] W.-G. Kim et al., "Triboelectric nanogenerator: Structure, mechanism, and applications," *ACS Nano*, vol. 15, no. 1, pp. 258–287, 2021.

[29] P. Bai et al., "Cylindrical rotating triboelectric nanogenerator," *ACS Nano*, vol. 7, no. 7, pp. 6361–6366, 2013.

[30] S. Niu et al., "Theoretical study of contact-mode triboelectric nanogenerators as an effective power source," *Energy Environ. Sci.*, vol. 6, no. 12, pp. 3576–3583, 2013.

[31] R. D. I. G. Dharmasena et al., "Triboelectric nanogenerators: Providing a fundamental framework," *Energy Environ. Sci.*, vol. 10, no. 8, pp. 1801–1811, 2017.

[32] Q.-Z. Guo and C.-P. Liu, "Derivation of analytical equations with experimental verification for working mechanism of triboelectric nanogenerators in contact-separation mode," *Nano Energy*, vol. 76, Oct. 2020, Art. no. 104969.

[33] S. Niu et al., "Theory of sliding-mode triboelectric nanogenerators," *Adv. Mater.*, vol. 25, no. 43, pp. 6184–6193, 2013.

[34] S. Niu et al., "Simulation method for optimizing the performance of an integrated triboelectric nanogenerator energy harvesting system," *Nano Energy*, vol. 8, pp. 150–156, Sep. 2014. [Online]. Available: https://www.sciencedirect.com/science/article/pii/S2211285514001025

[35] Y. Zi, S. Niu, J. Wang, Z. Wen, W. Tang, and Z. L. Wang, "Standards and figure-of-merits for quantifying the performance of triboelectric nanogenerators," *Nature Commun.*, vol. 6, no. 1, pp. 1–8, Sep. 2015.

[36] P. Yingyong, P. Thainiramit, S. Nundrakwang, P. Janphuang, and D. Isarakorn, "A comparative study of the electrical characteristics of piezoelectric and triboelectric nanogenerators for energy-harvesting floor tiles," in *Proc. 17th Int. Conf. Electr. Eng./Electron., Comput., Telecommun. Inf. Technol.*, Jun. 2020, pp. 9–12.

[37] D. Kwon, G. A. Rincon-Mora, and E. O. Torres, "Harvesting ambient kinetic energy with switched-inductor converters," *IEEE Trans. Circuits Syst. I, Reg. Papers*, vol. 58, no. 7, pp. 1551–1560, Jul. 2011.

[38] R. D. I. G. Dharmasena, "Inherent asymmetry of the current output in a triboelectric nanogenerator," *Nano Energy*, vol. 76, Oct. 2020, Art. no. 105045.

[39] E. Lefeuvre, A. Badel, C. Richard, and D. Guyomar, "Piezoelectric energy harvesting device optimization by synchronous electric charge extraction," *J. Intell. Mater. Syst. Struct.*, vol. 16, no. 10, pp. 865–876, Oct. 2005.

[40] E. Lefeuvre, "High-performance piezoelectric vibration energy reclamation," *Proc. SPIE*, vol. 5390, pp. 379–387, Jul. 2004.

[41] D. Zhao et al., "Universal equivalent circuit model and verification of current source for triboelectric nanogenerator," *Nano Energy*, vol. 89, Nov. 2021, Art. no. 106335.

[42] S. Niu, Y. Liu, Y. S. Zhou, S. Wang, L. Lin, and Z. L. Wang, "Optimization of triboelectric nanogenerator charging systems for efficient energy harvesting and storage," *IEEE Trans. Electron Devices*, vol. 62, no. 2, pp. 641–647, Feb. 2015.

[43] A. Tabesh and L. G. Fréchette, "A low-power stand-alone adaptive circuit for harvesting energy from a piezoelectric micropower generator," *IEEE Trans. Ind. Electron.*, vol. 57, no. 3, pp. 840–849, Mar. 2010.

[44] C. Peters, J. Handwerker, D. Maurath, and Y. Manoli, "A sub-500 mV highly efficient active rectifier for energy harvesting applications," *IEEE Trans. Circuits Syst. I, Reg. Papers*, vol. 58, no. 7, pp. 1542–1550, Jul. 2011.

[45] C. Peters, O. Kessling, F. Henrici, M. Ortmanns, and Y. Manoli, "CMOS integrated highly efficient full wave rectifier," in *Proc. IEEE Int. Symp. Circuits Syst.*, May 2007, pp. 2415–2418.

[46] G. D. Szarka, B. H. Stark, and S. G. Burrow, "Review of power conditioning for kinetic energy harvesting systems," *IEEE Trans. Power Electron.*, vol. 27, no. 2, pp. 803–815, Feb. 2012.

[47] P. W. Yuen, G. Chong, and H. Ramiah, "A high efficient dual-output rectifier for piezoelectric energy harvesting," *AEU-Int. J. Electron. Commun.*, vol. 111, Nov. 2019, Art. no. 152922.

[48] J. Nunez and M. J. Avedillo, "Reducing the impact of reverse currents in tunnel FET rectifiers for energy harvesting applications," *IEEE J. Electron Devices Soc.*, vol. 5, no. 6, pp. 530–534, Nov. 2017.

[49] T. H. Saika and M. T. Amin, "A high efficient wide range cross coupled rectifier for RFID applications," in *Proc. Int. Conf. Comput., Electr. Commun. Eng. (ICCECE)*, Jan. 2020, pp. 1–6.

[50] A. Hirono, Y. Muramoto, S. Tsuchimoto, N. Sakai, and K. Itoh, "The 2.4 GHz band SOI-CMOS high power bridge rectifier IC with the cross coupled CMOS pair," in *Proc. IEEE Wireless Power Transf. Conf. (WPTC)*, Jun. 2021, pp. 1–4.

[51] J. S. Y. Tan et al., "A fully energy-autonomous temperature-to-time converter powered by a triboelectric energy harvester for biomedical applications," *IEEE J. Solid-State Circuits*, vol. 56, no. 10, pp. 2913–2923, Oct. 2021.

[52] J. Lee et al., "A triboelectric energy-harvesting interface with scalable multi-chip-stacked bias-flip and daisy-chained synchronous signaling techniques," *IEEE J. Solid-State Circuits*, vol. 57, no. 12, pp. 1–15, Apr. 2022.

[53] S. Niu, X. Wang, F. Yi, Y. S. Zhou, and Z. L. Wang, "A universal self-charging system driven by random biomechanical energy for sustainable operation of mobile electronics," *Nature Commun.*, vol. 6, no. 1, pp. 3825–3839, Dec. 2015.

[54] Y. Zhang et al., "Flexible transparent high-voltage diodes for energy management in wearable electronics," *Nano Energy*, vol. 40, pp. 289–299, Oct. 2017.

[55] I. Park et al., "A high-voltage dual-input buck converter achieving 52.9% maximum end-to-end efficiency for triboelectric energy-harvesting applications," *IEEE J. Solid-State Circuits*, vol. 55, no. 5, pp. 1324–1336, May 2020.

[56] I.-Y. Park et al., "BCD (bipolar-CMOS-DMOS) technology trends for power management IC," in *Proc. 8th Int. Conf. Power Electron.*, May 2011, pp. 318–325.

[57] I. Park, J. Maeng, D. Lim, M. Shim, J. Jeong, and C. Kim, "A 4.5-to-16μW integrated triboelectric energy-harvesting system based on high-voltage dual-input buck converter with MPPT and 70 V maximum input voltage," in *IEEE Int. Solid-State Circuits Conf. (ISSCC) Dig. Tech. Papers*, Feb. 2018, pp. 146–148.

[58] I. Park, J. Maeng, M. Shim, J. Jeong, and C. Kim, "A bidirectional high-voltage dual-input buck converter for triboelectric energy-harvesting interface achieving 70.72% end-to-end efficiency," in *Proc. Symp. VLSI Circuits*, Jun. 2019, pp. C326–C327.

[59] J. Maeng, I. Park, M. Shim, J. Jeong, and C. Kim, "A high-voltage dual-input buck converter with bidirectional inductor current for triboelectric energy-harvesting applications," *IEEE J. Solid-State Circuits*, vol. 56, no. 2, pp. 541–553, Feb. 2021.

[60] A. Ghaffarinejad, J. Y. Hasani, D. Galayko, and P. Basset, "Superior performance of half-wave to full-wave rectifier as a power conditioning circuit for triboelectric nanogenerators: Application to contact-separation and sliding mode TENG," *Nano Energy*, vol. 66, Dec. 2019, Art. no. 104137. [Online]. Available: https://www.sciencedirect.com/science/article/pii/S2211285519308444

[61] Y. K. Ramadass and A. P. Chandrakasan, "An efficient piezoelectric energy harvesting interface circuit using a bias-flip rectifier and shared inductor," *IEEE J. Solid-State Circuits*, vol. 45, no. 1, pp. 189–204, Jan. 2010.

[62] J. McCullagh, "An active diode full-wave charge pump for low acceleration infrastructure-based non-periodic vibration energy harvesting," *IEEE Trans. Circuits Syst. I, Reg. Papers*, vol. 65, no. 5, pp. 1758–1770, May 2018.

[63] N. A. K. Z. Abidin, N. M. Nayan, M. M. Azizan, and A. Ali, "Analysis of voltage multiplier circuit simulation for rain energy harvesting using circular piezoelectric," *Mech. Syst. Signal Process.*, vol. 101, pp. 211–218, Feb. 2018.

[64] B. Axelrod and Y. Berkovich, "Cockroft–Walton voltage multiplier combined with switched-coupled-inductor boost converter," in *Proc. IEEE Int. Energy Conf.*, Apr. 2016, pp. 1–5.

[65] X. Liu et al., "Alternating current electroluminescent device powered by triboelectric nanogenerator with capacitively driven circuit strategy," *Adv. Funct. Mater.*, vol. 32, no. 7, Feb. 2022, Art. no. 2106411.

[66] A. C. M. de Queiroz and M. Domingues, "The doubler of electricity used as battery charger," *IEEE Trans. Circuits Syst. II, Exp. Briefs*, vol. 58, no. 12, pp. 797–801, Dec. 2011.

[67] A. Ghaffarinejad et al., "A conditioning circuit with exponential enhancement of output energy for triboelectric nanogenerator," *Nano Energy*, vol. 51, pp. 173–184, Sep. 2018.

[68] A. C. M. de Queiroz, "Electrostatic vibrational energy harvesting using a variation of Bennet's doubler," in *Proc. 53rd IEEE Int. Midwest Symp. Circuits Syst.*, Aug. 2010, pp. 404–407.

[69] B. D. Truong, C. P. Le, and E. Halvorsen, "Analysis of electrostatic energy harvesters electrically configured as Bennet's doublers," *IEEE Sensors J.*, vol. 17, no. 16, pp. 5180–5191, Aug. 2017.

[70] V. P. Dragunov, V. Y. Dorzhiev, D. I. Ostertak, and V. V. Atuchin, "A new autostabilization mechanism in the Bennet doubler circuit-based electrostatic vibrational energy harvester," *Sens. Actuators A, Phys.*, vol. 272, pp. 259–266, Apr. 2018. [Online]. Available: https://www.sciencedirect.com/science/article/pii/S0924424717315807

[71] V. P. Dragunov, D. I. Ostertak, and R. E. Sinitskiy, "New modifications of a Bennet doubler circuit-based electrostatic vibrational energy harvester," *Sens. Actuators A, Phys.*, vol. 302, Feb. 2020, Art. no. 111812.

[72] A. Karami, D. Galayko, and P. Basset, "Series-parallel charge pump conditioning circuits for electrostatic kinetic energy harvesting," *IEEE Trans. Circuits Syst. I, Reg. Papers*, vol. 64, no. 1, pp. 227–240, Jan. 2017.

[73] H. Zhang, D. Galayko, and P. Basset, "A conditioning system for high-voltage electrostatic/triboelectric energy harvesters using Bennet doubler and self-actuated hysteresis switch," in *Proc. 20th Int. Conf. Solid-State Sensors, Actuat. Microsyst. Eurosensors*, Jun. 2019, pp. 346–349.

[74] H. Zhang, F. Marty, D. Galayko, N. Hodzic, and P. Basset, "High-voltage MEMS plasma switch for boosting the energy transfer efficiency in triboelectric nanogenerators," in *Proc. IEEE 33rd Int. Conf. Micro Electro Mech. Syst. (MEMS)*, Jan. 2020, pp. 610–613.

[75] M. A. B. Ouanes, H. Samaali, D. Galayko, P. Basset, and F. Najar, "A new type of triboelectric nanogenerator with self-actuated series-to-parallel electrical interface based on self-synchronized mechanical switches for exponential charge accumulation in a capacitor," *Nano Energy*, vol. 62, pp. 465–474, Aug. 2019.

[76] H. Zhang, Y. Lu, A. Ghaffarinejad, and P. Basset, "Progressive contact-separate triboelectric nanogenerator based on conductive polyurethane foam regulated with a Bennet doubler conditioning circuit," *Nano Energy*, vol. 51, pp. 10–18, Sep. 2018.

[77] D. Morel et al., "A shock-optimized SECE integrated circuit," *IEEE J. Solid-State Circuits*, vol. 53, no. 12, pp. 3420–3433, Dec. 2018.

[78] X. Cheng et al., "High efficiency power management and charge boosting strategy for a triboelectric nanogenerator," *Nano Energy*, vol. 38, pp. 438–446, Aug. 2017.

[79] F. Xi et al., "Universal power management strategy for triboelectric nanogenerator," *Nano Energy*, vol. 37, pp. 168–176, Jul. 2017.

[80] H. Qin et al., "High energy storage efficiency triboelectric nanogenerators with unidirectional switches and passive power management circuits," *Adv. Funct. Mater.*, vol. 28, no. 51, Dec. 2018, Art. no. 1805216.

[81] J. Yang et al., "Managing and optimizing the output performances of a triboelectric nanogenerator by a self-powered electrostatic vibrator switch," *Nano Energy*, vol. 46, pp. 220–228, Apr. 2018.

[82] M. Pathak, S. Xie, C. Huang, and R. Kumar, "High-voltage triboelectric energy harvesting using multi-shot energy extraction in 70-V BCD process," *IEEE Trans. Circuits Syst. II, Exp. Briefs*, vol. 69, no. 5, pp. 2513–2517, May 2022.

[83] Y. Zi et al., "Effective energy storage from a triboelectric nanogenerator," *Nature Commun.*, vol. 7, no. 1, pp. 1–8, Mar. 2016.

[84] A. Morel, P. Gasnier, Y. Wanderoild, G. Pillonnet, and A. Badel, "Short circuit synchronous electric charge extraction (SC-SECE) strategy for wideband vibration energy harvesting," in *Proc. IEEE Int. Symp. Circuits Syst. (ISCAS)*, May 2018, pp. 1–5.

[85] A. Morel et al., "Fast-convergence self-adjusting SECE circuit with tunable short-circuit duration exhibiting 368% bandwidth improvement," *IEEE Solid-State Circuits Lett.*, vol. 3, pp. 222–225, 2020.

[86] I. C. Lien, Y. C. Shu, W. J. Wu, S. M. Shiu, and H. C. Lin, "Revisit of series-SSHI with comparisons to other interfacing circuits in piezoelectric energy harvesting," *Smart Mater. Struct.*, vol. 19, no. 12, 2010, Art. no. 125009.

[87] D. A. Sanchez, J. Leicht, F. Hagedorn, E. Jodka, E. Fazel, and Y. Manoli, "A parallel-SSHI rectifier for piezoelectric energy harvesting of periodic and shock excitations," *IEEE J. Solid-State Circuits*, vol. 51, no. 12, pp. 2867–2879, Dec. 2016.

[88] L. Wu and D. S. Ha, "A self-powered piezoelectric energy harvesting circuit with an optimal flipping time SSHI and maximum power point tracking," *IEEE Trans. Circuits Syst. II, Exp. Briefs*, vol. 66, no. 10, pp. 1758–1762, Oct. 2019.

[89] S. Fang et al., "An efficient piezoelectric energy harvesting circuit with series-SSHI rectifier and FNOV-MPPT control technique," *IEEE Trans. Ind. Electron.*, vol. 68, no. 8, pp. 7146–7155, Aug. 2021.

[90] H. Xia et al., "A self-powered S-SSHI and SECE hybrid rectifier for PE energy harvesters: Analysis and experiment," *IEEE Trans. Power Electron.*, vol. 36, no. 2, pp. 1680–1692, Feb. 2021.

[91] X. Li and Y. Sun, "An SSHI rectifier for triboelectric energy harvesting," *IEEE Trans. Power Electron.*, vol. 35, no. 4, pp. 3663–3678, Apr. 2020.

[92] I. Kara, M. Becermis, M. A.-A. Kamar, M. Aktan, H. Dogan, and S. Mutlu, "A 70-to-2 V triboelectric energy harvesting system utilizing parallel-SSHI rectifier and DC–DC converters," *IEEE Trans. Circuits Syst. I, Reg. Papers*, vol. 68, no. 1, pp. 210–223, Jan. 2021.

[93] L. Jiho et al., "A 130 V triboelectric energy-harvesting interface in 0.18 μm BCD with scalable multi-chip-stacked bias-flip and daisy-chained synchronous signaling technique," in *IEEE Int. Solid-State Circuits Conf. (ISSCC) Dig. Tech. Papers*, Feb. 2022, pp. 474–476.

[94] S. H. Lee et al., "A rectifier-reusing bias-flip energy harvesting interface circuit with adaptively reconfigurable SC converter for wind-driven triboelectric nanogenerator," *IEEE Trans. Ind. Electron.*, vol. 70, no. 8, pp. 8022–8031, Aug. 2022.

[95] S. Javvaji, V. Singhal, V. Menezes, R. Chauhan, and S. Pavan, "Analysis and design of a multi-step bias-flip rectifier for piezoelectric energy harvesting," *IEEE J. Solid-State Circuits*, vol. 54, no. 9, pp. 2590–2600, Sep. 2019.

[96] Z. Chen, M.-K. Law, P.-I. Mak, W.-H. Ki, and R. P. Martins, "A 1.7 mm^2 inductorless fully integrated flipping-capacitor rectifier (FCR) for piezoelectric energy harvesting with 483% power-extraction enhancement," in *IEEE Int. Solid-State Circuits Conf. (ISSCC) Dig. Tech. Papers*, Feb. 2017, pp. 372–373.

[97] S. Du and A. A. Seshia, "An inductorless bias-flip rectifier for piezoelectric energy harvesting," *IEEE J. Solid-State Circuits*, vol. 52, no. 10, pp. 2746–2757, Oct. 2017.

[98] Z. Chen, M.-K. Law, P.-I. Mak, X. Zeng, and R. P. Martins, "Piezoelectric energy-harvesting interface using split-phase flipping-capacitor rectifier with capacitor reuse for input power adaptation," *IEEE J. Solid-State Circuits*, vol. 55, no. 8, pp. 2106–2117, Aug. 2020.

[99] X. Yue and S. Du, "Voltage flip efficiency optimization of SSHC rectifiers for piezoelectric energy harvesting," in *Proc. IEEE Int. Symp. Circuits Syst. (ISCAS)*, May 2021, pp. 1–5.

[100] W. Tang, T. Zhou, C. Zhang, F. R. Fan, C. B. Han, and Z. L. Wang, "A power-transformed-and-managed triboelectric nanogenerator and its applications in a self-powered wireless sensing node," *Nanotechnology*, vol. 25, no. 22, Jun. 2014, Art. no. 225402.

[101] Y. Yoon et al., "A continuously-scalable-conversion-ratio step-up/down SC energy-harvesting interface with MPPT enabled by real-time power monitoring with frequency-mapped capacitor DAC," *IEEE Trans. Circuits Syst. I, Reg. Papers*, vol. 69, no. 4, pp. 1820–1831, Apr. 2022.

[102] Y. Zi et al., "An inductor-free auto-power-management design built-in triboelectric nanogenerators," *Nano Energy*, vol. 31, pp. 302–310, Jan. 2017.

[103] W. Liu et al., "Switched-capacitor-convertors based on fractal design for output power management of triboelectric nanogenerator," *Nature Commun.*, vol. 11, no. 1, p. 1883, Apr. 2020.

[104] S. Zargari, A. Rezania, Z. D. Koozehkanani, H. Veladi, J. Sobhi, and L. Rosendahl, "Effect of the inherent capacitance optimization on the output performance of triboelectric nanogenerators," *Nano Energy*, vol. 92, Feb. 2022, Art. no. 106740.

[105] A. M. El-Mohandes and R. Zheng, "Active matching circuit to enhance the generated power of triboelectric nanogenerators," *Nano Energy*, vol. 80, Feb. 2021, Art. no. 105588.

[106] L. Costanzo, A. Lo Schiavo, and M. Vitelli, "Active interface for piezoelectric harvesters based on multi-variable maximum power point tracking," *IEEE Trans. Circuits Syst. I, Reg. Papers*, vol. 67, no. 7, pp. 2503–2515, Jul. 2020.

[107] P. Laurent, J.-F. Fagnard, F. Dupont, and J.-M. Redoute, "Optimization of the power flow generated by an AC energy harvester for variable operating conditions," *IEEE Trans. Circuits Syst. I, Reg. Papers*, vol. 69, no. 6, pp. 2625–2636, Jun. 2022.

[108] M. Dini, A. Romani, M. Filippi, V. Bottarel, G. Ricotti, and M. Tartagni, "A nanocurrent power management IC for multiple heterogeneous energy harvesting sources," *IEEE Trans. Power Electron.*, vol. 30, no. 10, pp. 5665–5680, Oct. 2015.

[109] M. Pathak and R. Kumar, "Synchronous inductor switched energy extraction circuits for triboelectric nanogenerator," *IEEE Access*, vol. 9, pp. 76938–76954, 2021.

[110] S. Li, A. Roy, and B. H. Calhoun, "A piezoelectric energy-harvesting system with parallel-SSHI rectifier and integrated maximum-power-point tracking," *IEEE Solid-State Circuits Lett.*, vol. 2, no. 12, pp. 301–304, Dec. 2019.

[111] M. Pathak and R. Kumar, "Pre-biased synchronous charge extraction for triboelectric nanogenerator," in *Proc. IEEE Sensors*, Oct. 2019, pp. 1–4.

[112] J. Chen et al., "Self-powered pumping switched TENG enabled real-time wireless metal tin height and position recognition and counting for production line management," *Nano Energy*, vol. 90, Dec. 2021, Art. no. 106544. [Online]. Available: https://www.sciencedirect.com/science/article/pii/S2211285521007965

[113] Y. Li et al., "Low-cost, environmentally friendly, and high-performance triboelectric nanogenerator based on a common waste material," *ACS Appl. Mater. Interface*, vol. 13, no. 26, pp. 30776–30784, Jul. 2021.

[114] W. Harmon, D. Bamgboje, H. Guo, T. Hu, and Z. L. Wang, "Self-driven power management system for triboelectric nanogenerators," *Nano Energy*, vol. 71, May 2020, Art. no. 104642.

[115] K. Rawy, R. Sharma, H.-J. Yoon, U. Khan, S.-W. Kim, and T. T. Kim, "An 88% efficiency 2.4μW to 15.6μW triboelectric nanogenerator energy harvesting system based on a single-comparator control algorithm," in *Proc. IEEE Asian Solid-State Circuits Conf. (A-SSCC)*, Nov. 2018, pp. 33–36.

[116] B. Ciftci, S. Chamanian, A. Koyuncuoglu, A. Muhtaroglu, and H. Kulah, "A low-profile autonomous interface circuit for piezoelectric micro-power generators," *IEEE Trans. Circuits Syst. I, Reg. Papers*, vol. 68, no. 4, pp. 1458–1471, Apr. 2021.

Wenyu Peng (Student Member, IEEE) received the B.Sc. degree from the Glasgow College, University of Electronic Science and Technology of China (UESTC), in 2020, and the M.Sc. degree from the Department of Microelectronics, Electronic Instrumentation Section, Delft University of Technology (TU Delft), The Netherlands, in February 2023, where he is currently pursuing the Ph.D. degree with the Department of Microelectronics. His current research interests include triboelectric and multi-source energy harvesting for wearable and the biomedical and Internet of Things (IoT) autonomous sensors, including energy-efficient power management circuit designs and front-end harvester fabrications.

Sijun Du (Senior Member, IEEE) received the B.Eng. degree (Hons.) in electrical engineering from University Pierre and Marie Curie (UPMC), Paris, France, in 2011, the M.Sc. degree (Hons.) in electrical and electronics engineering from the Imperial College London, London, U.K., in 2012, and the Ph.D. degree in electrical engineering from the University of Cambridge, Cambridge, U.K., in January 2018.

He started his Ph.D. research in October 2014. He worked with Laboratoire d'Informatique de Paris 6 (LIP6), UPMC, and then worked as a Digital IC Engineer, Shanghai, China, from 2012 to 2014. He was a Summer Engineer Intern with Qualcomm Technology Inc., San Diego, CA, USA, in 2016. He was a Visiting Scholar with the Department of Microelectronics, Fudan University, Shanghai, China, in 2018. He was a Post-Doctoral Researcher with the Berkeley Wireless Research Center (BWRC), Department of Electrical Engineering and Computer Sciences (EECS), University of California at Berkeley, Berkeley, CA, USA, from 2018 to 2020. In 2020, he joined the Department of Microelectronics, Delft University of Technology (TU Delft), Delft, The Netherlands, where he is currently a tenured Assistant Professor. His current research interests include energy-efficient integrated circuits and systems, including power management integrated circuits (PMIC), energy harvesting, wireless power transfer, DC/DC converters used in Internet of Things (IoT) wireless sensors, wearable electronics, biomedical devices, and microrobots.

Dr. Du received the Dutch Research Council (NWO) Talent Program-VENI grant in 2021. He was a co-recipient of the Best Student Paper Award in IEEE ICECS 2022. He is a Technical Committee Member of the IEEE Power Electronics Society (PELS) and IEEE Circuits and Systems Society (CASS). He served as the Sub-Committee Chair for IEEE ICECS 2022, a Review Committee Member for IEEE ISCAS from 2021 to 2023, and a Committee Member for the 2023 IEEE ISSCC Student Research Preview (SRP).